

Assembling SnO Nanosheets into Microhydrangeas: Gas Phase Synthesis and Their Optical Property

Zhenglin Zhang^{1,2}, Jing Wang¹, Zhou Yu¹, Fengyu Qu¹, Xiang Wu^{1,2,*}

(Received 25 September 2012; accepted 4 November 2012; published online 10 November 2012.)

Abstract: Large scale SnO microhydrangeas are obtained successfully through thermally evaporating of SnO₂ powder wrapped by a filter paper at 1050°C and using gold coated Si wafer as the substrate. The as-obtained SnO microhydrangeas are consisted of many thin nanosheets with the thicknesses of 30-60 nm and the diameters of 500-600 nm. A vapor-liquid-solid (VLS) growth mechanism for the as-synthesized SnO microhydrangeas was proposed based on experimental results. Photoluminescence spectrum (PL) shows that there is a strong sharp ultraviolet emission peak at 390 nm, revealing that these three-dimensional SnO microhydrangeas may have potential applications in optoelectronic fields.

Keywords: SnO; microhydrangeas; Photoluminescence; VLS

Citation: Zhenglin Zhang, Jing Wang, Zhou Yu, Fengyu Qu and Xiang Wu, "Assembling SnO Nanosheets into Microhydrangeas: Gas Phase Synthesis and Their Optical Property", Nano-Micro Lett. 4 (4), 215-219 (2012). <http://dx.doi.org/10.3786/nml.v4i4.p215-219>

To design rationally the desired nanostructures with the controlled size and shape is a key step toward the future nanotechnological applications. SnO and SnO₂ are two important wide band gap semiconductors. Tin dioxide (SnO₂, $E_g = 3.62$ eV, at 300 K) has been widely studied due to its promising applications in gas sensors [1-3], solar cells [4], optical devices [5-6], lithium ion batteries [7-8], and photocatalysts [9-11]. In contrast, the investigation of SnO materials has fallen behind, perhaps because it decomposes easily at elevated temperature and the divalent tin ion can be oxidized to the tetravalent one. However, as is known, SnO is technologically important as a p-type semiconductor, which is a key functional material that has been widely studied for various potential applications [12]. In the past few decades, many SnO crystals with uniform nanostructures are obtained including sheets [13], wires [14], diskettes [15], and nanoribbons [16]. Those

materials have been widely explored for rechargeable lithium batteries [17-18], and storage of solar energy [19]. However, synthesis of hydrangealike SnO structure with thin nanosheet assemblies is rarely reported [20].

In the present work, we present a simply Thermally vapor deposition approach for the controlled growth of SnO microhydrangeas. Morphologies and optical property of the as-synthesized products are investigated by different characterization techniques. The growth mechanism was also proposed.

SnO microhydrangeas were synthesized using a facile chemical vapor deposition (CVD) method in a conventional horizontal tube furnace (inner diameter 40 mm, length 70 cm, see Fig. 1(c)). The Si substrates were covered with a layer of Au film of about 5 nm. First, the substrates were immersed into acetone and ethanol in succession, washed ultrasonically for 15 minutes and

¹Key Laboratory for Photonic and Electronic Bandgap Materials, Ministry of Education and College of Chemistry and Chemical Engineering, Harbin Normal University, Harbin, 150025, P. R. China

²Key Laboratory of Colloid and Interface Chemistry, Ministry of Education and College of Chemistry and Chemical Engineering, Shandong University, Jinan, 250100, Shandong, P. R. China.

*Corresponding author. E-mail: wuxiang05@gmail.com

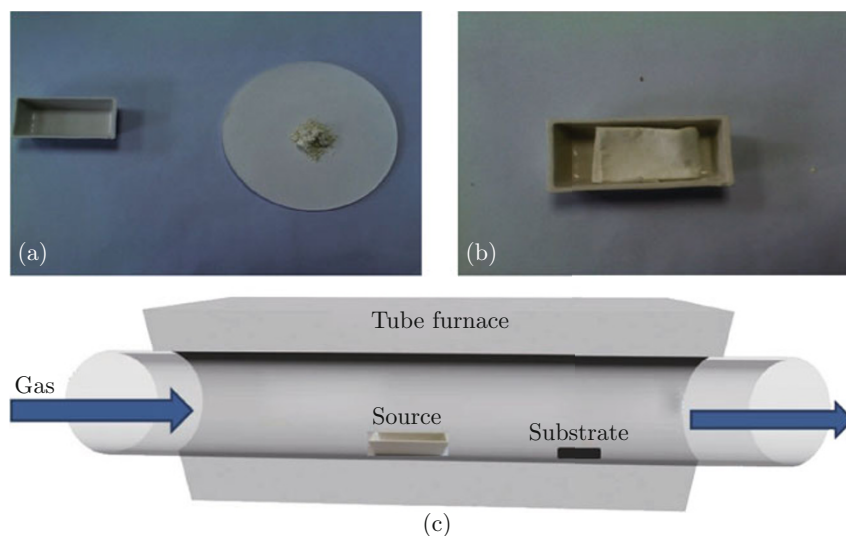


Fig. 1 (a-b) Digital photographs of the filter paper wrapped SnO_2 power and the boat. (c) Schematic illustration of experimental setup to synthesize the SnO nanostructures.

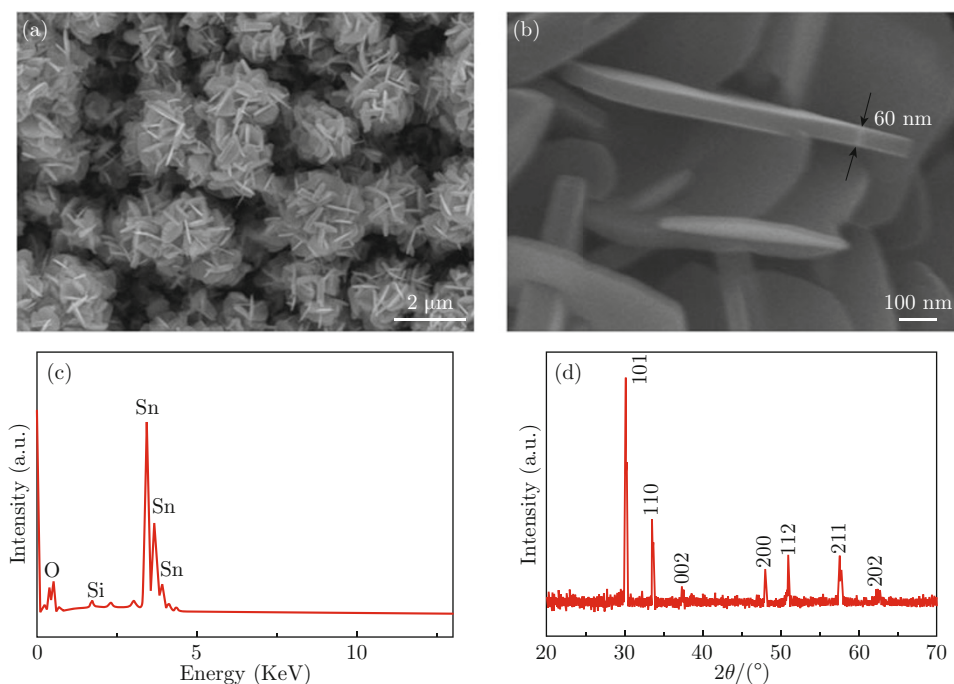


Fig. 2 Morphology of the as-synthesized SnO microhydrangeas. (a-b) SEM images at different magnifications. (c) Energy-dispersive spectrum (EDS) recorded from SnO microhydrangeas. (d) XRD pattern of the as-obtained SnO nanostructures.

rinsed with deionized water, then dried by a drier. The substrates were placed downstream, which are 21 cm away from the source material. 1 g SnO_2 (99.98% purity) was tightly wrapped by a filter paper (Fig. 1(a)-(b)), and was put into an alumina boat. Then, the boat was taken into the horizontal tube furnace. Subsequently, the whole system was evacuated for 30 min by a vacuum pump. The temperature was rapidly increased from room temperature up to 1050°C and kept 1 h at this temperature. Carrier of argon flowed into the tube at the rate of 100 sccm, and the pressure was

kept at 10 Torr. Finally, the furnace was cooled down room temperature. The substrates were taken out from the tube. The as-synthesized products were characterized by X-ray diffraction instrument (Rigaku Dmax-rB, $\text{CuK}\alpha$ radiation, $\lambda = 0.1542$ nm, 40 KV, 100 mA), scanning electron microscope (SEM, Hitachi-4800), micro-Raman spectrometer (HR800) and Photoluminescence spectrum (HORIBA JY-Fluoro Max 4).

Morphology of the as-synthesized product is characterized firstly by SEM. A typical low magnification SEM image is shown in Fig. 2(a), revealing large quan-

ties of hydrangealike structures with average diameters of 2-3 μm . Figure 2(b) shows a high magnification SEM image of the as-synthesized products, which are consisted of some nanosheets with smooth surfaces with the average thicknesses of 60 nm. The energy dispersive X-ray spectrum (EDS) of the as-synthesized nanostructure is shown in Fig. 2(c), EDS quantitative analysis gives an average Sn/O ratio of 40.88:59.12 within the accuracy of the technique. The peaks for Sn and O are originated from the source material. Si element is from the substrate. Figure 2d shows XRD pattern of the as-synthesized products. All of the diffraction peaks can be indexed to a tetragonal SnO structure (JCPDS Card No.06-0395), with lattice constants of $a=3.796 \text{ \AA}$ and $c=4.816 \text{ \AA}$. The sharp and strong diffraction peaks indicate that the as-synthesized SnO hydrangealike nanostructures are highly crystalline.

Raman spectrograph is utilized to further study the microstructure of the as-synthesized product. Figure 3 shows a Raman scattering spectrum of the as-obtained hydrangealike microstructure at room temperature. Four major vibration peaks located at 80, 107, 138 and 207 cm^{-1} can be found. The Raman spectrum exhibits two Raman modes at 113 cm^{-1} (E_{1g}) and 211 cm^{-1} (A_{1g}) in previous report [21]. Besides these typical Raman modes, the other two peaks at 80 and 138 cm^{-1} are assigned as B_{1g} mode and E_{2g} mode, respectively. These peaks further confirm that the SnO nanostructures possess the characteristics of the tetragonal SnO structure [22].

To investigate the growth mechanism of the as-obtained SnO microhydrangeas, temperature dependent experiments are conducted. In Fig. 4(a), only a

small quantity of nanosheets were observed for 1 min. Adding time to 30 min (in Fig. 4(b)), it was found that large quantities of nanosheets with a relative smooth surfaces deposited on the substrate. However, it is not assembled to microhydrangeas. When increasing to 1 h at the temperature, many hydrangealike structures appeared, as shown in Fig. 4(c).

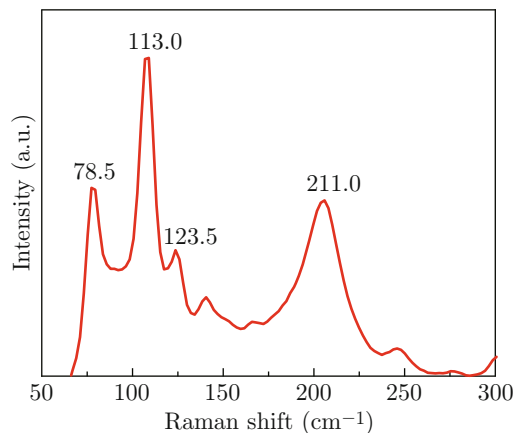


Fig. 3 Raman spectrum of the as-synthesized product.

Experiment results indicated that growth of the as-synthesized product can be explained by a vapor-liquid-solid (VLS) mechanism. Figure 5 shows a growth schematic drawing of the SnO microhydrangeas. In the experiment, we suggest that the filter paper (main ingredient is cellulose ($\text{C}_6\text{H}_{10}\text{O}_5$) $_n$) will be a direct reacting substance at the begin of the reaction. In situ carbon is obtained by heating the paper to more than

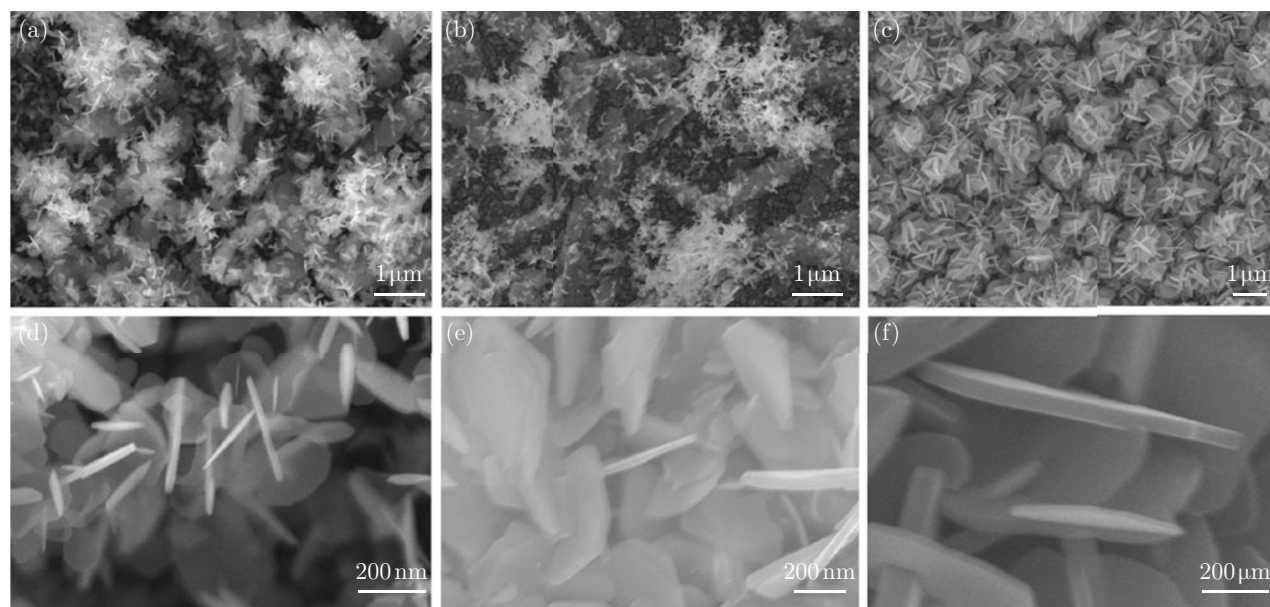


Fig. 4 SEM images of the SnO nanostructures by using different reaction time for 1050°C: (a, d) 1 min, (b, e) 30 min, (c, f) 1 h.

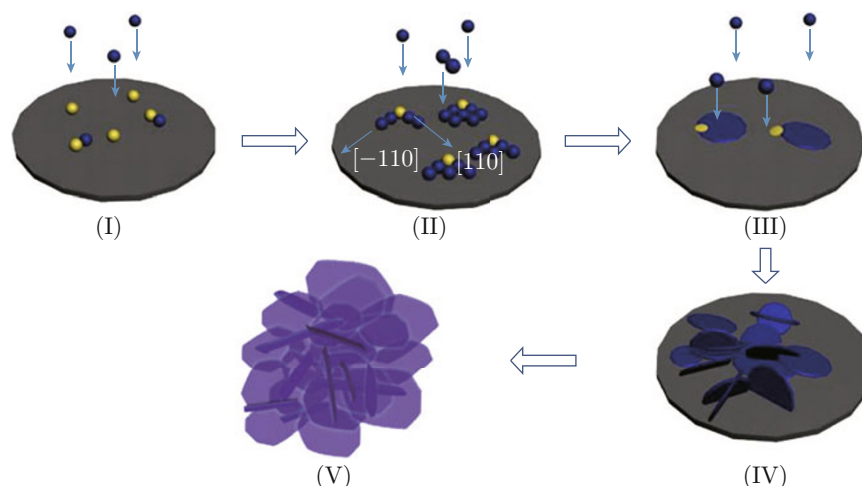


Fig. 5 Growth Schematic drawing of the as-synthesized SnO nanostructures: (I) Metallic tin droplets dissolve with Au nanoparticles. (II) SnO nuclei grows along the [110] and [-110] crystal directions. (III) Nanosheets form (IV) a mass of SnO nanosheets form with reaction proceeds. (V) the nanosheets assemble into microhydrangeas.

150°C, and the carbon has more exceptional reduction ability than pure graphite or other carbon material.

Next, as the temperature is elevated, the following chemical reactions occur:



In reaction 1, SnO vapors and CO gas are generated in high temperature region of the tube furnace. The reaction products were then transported downstream by the Ar gas flow, where reaction 2 shall occur. Sn vapor can be dissolved in Au nanoparticle catalyst to form Sn-Au alloy. When solubility of the Sn vapor in the Au nanoparticle reaches supersaturated, Sn can overflow from the Au nanoparticle catalyst and react with residual oxygen in the closed system to form SnO nuclei at the catalyst interface [23, 24]. The tetragonal phase SnO structure are preferentially oriented along the [110] and [-110] growth directions. With the reaction progress, SnO nuclei can assemble into SnO nanosheets and further microhydrangeas. No Au particles have been found on tops of the obtained nanosheets, which probably have been evaporated during the growth of the SnO nanosheets, this explanation is consisted with ZnO and MgB₂ nanohelices [25, 26].

Room temperature photoluminescence (PL) spectrum of the obtained SnO microstructures are measured with UV light excitation at 300 nm. Figure 6 shows single and strong emission spectra at 390 nm (3.18 eV), no obvious other emission peak can be found. SnO with the tetragonal structure is a p-type semiconductor with a wide optical band gap of 2.7-3.4 eV. So, the ultraviolet PL peak at 390 nm (3.18 eV) is possibly attributed to the band edge emission of SnO [20]. In literature, SnO thin films exhibited a broad dominant peak near 396 nm (3.13 eV) [27]. It suggests the quantum-confinement ef-

fect in SnO nanostructures induces a blue-shift of the absorption band [14].

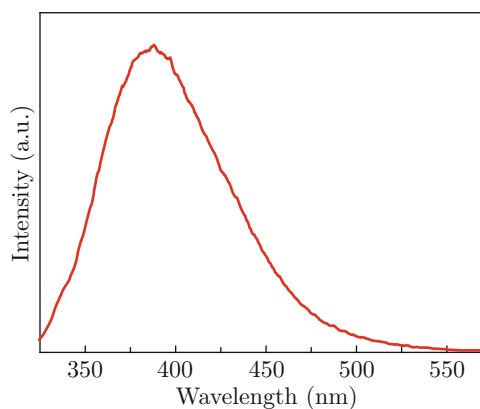


Fig. 6 Photoluminescence spectrum of the as-obtained SnO nanostructures.

In summary, large quantities of SnO microhydrangeas through assembling nanosheets are successfully synthesized though a CVD method. A possible growth mechanism based VLS growth for the as-synthesized product is proposed. Photoluminescence spectrum measurement showed a strong emission peak at 390 nm, which may be ascribed to band edge emission, and expected to be the promising candidate in optoelectronics micro/nanodevices.

Acknowledgements

This work was sponsored by China Postdoctoral Foundation (2012M511016), Special Fund of Postdoctoral Innovation Projects in Shandong Province (201201007), Postdoctoral Initiation Foundation of Shandong University and the Foundation for Key Project of Ministry of Education, China (No. 211046)

References

- [1] C. N. Xu, J. Tamaki, N. Miura and N. Yamazoe, *Sens. Actuators B* 3, 147 (1991). [http://dx.doi.org/10.1016/0925-4005\(91\)80207-Z](http://dx.doi.org/10.1016/0925-4005(91)80207-Z)
- [2] Y. L. Wang, X. C. Jiang and Y. N. Xia, *J. Am. Chem. Soc.* 125, 16176 (2003). <http://dx.doi.org/10.1021/ja037743f>
- [3] A. Kolmakov, D. O. Klenov, Y. Lilach, S. Stemmer and M. Moskovits, *Nano Lett.* 5, 667 (2005). <http://dx.doi.org/10.1021/nl050082v>
- [4] F. G. Fagan and V. R. Amarakoon, *Am. Ceram. Soc. Bull.* 72, 119 (1993).
- [5] Y. T. Han, X. Wu, G. Z. Shen, B. Dierre, L. H. Gong, F.Y. Qu, Y. Bando, T. Sekiguchi, F. Fabbri, and D. Golberg, *J. Phys. Chem. C* 114, 8235 (2010). <http://dx.doi.org/10.1021/jp100942m>
- [6] Q. H. Wang, D. W. Wang and T. M. Wang, *Nano-Micro Lett.* 3, 34 (2011). <http://dx.doi.org/10.3786/nml.v3i1.p34-42>
- [7] Y. Wang, F. Su, J. Y. Lee and X. S. Zhao, *Chem. Mater.* 18, 1347 (2006). <http://dx.doi.org/10.1021/cm052219o>
- [8] C. J. Kim, M. J. Noh, M. S. Choi, J. Cho and B. W. Park, *Chem. Mater.* 17, 3297 (2005). <http://dx.doi.org/10.1021/cm048003o>
- [9] B. X. Jia, W. N. Jia, Y. L. Ma, X. Wu and F. Y. Qu, *Sci. Adv. Mater.* 4, 702 (2012). <http://dx.doi.org/10.1166/sam.2012.1341>
- [10] H. T. Huang, S. Q. Tian, J. Xu, Z. Xie, D. W. Zeng, D. Chen and G. Z. Shen, *Nanotechnology* 23, 105502 (2012). <http://dx.doi.org/10.1088/0957-4484/23/10/105502>
- [11] Y. H. Han, X. Wu, Y. L. Ma, L. H. Gong, F. Y. Qu and H. J. Fan, *Cryst. Eng. Comm.* 13, 3506 (2011). <http://dx.doi.org/10.1039/c1ce05171g>
- [12] Y. Ogo, H. Hiramatsu, K. Nomura, H. Yanagi, T. Kamiya, M. Hirano and H. Hosono, *Appl. Phys. Lett.* 93, 032113 (2008). <http://dx.doi.org/10.1063/1.2964197>
- [13] K. Sakaushi, Y. Oaki, H. Uchiyama, E. Hosono, H. S. Zhou and H. Imai, *Small* 6, 776 (2010). <http://dx.doi.org/10.1002/smll.200902207>
- [14] K. Sakaushi, Y. Oaki, H. Uchiyama, E. Hosono, H. S. Zhou and H. Imai, *Nanoscale* 2, 2424 (2010). <http://dx.doi.org/10.1039/c0nr00370k>
- [15] Z. R. Dai, Z. W. Pan and Z. L. Wang, *J. Am. Chem. Soc.* 124, 8673 (2002). <http://dx.doi.org/10.1021/ja026262d>
- [16] Z. L. Wang and Z. W. Pan, *Adv. Mater.* 14, 1029 (2002). [http://dx.doi.org/10.1002/1521-4095\(20020805\)14:15<1029::AID-ADMA1029>3.0.CO;2-3](http://dx.doi.org/10.1002/1521-4095(20020805)14:15<1029::AID-ADMA1029>3.0.CO;2-3)
- [17] D. Aurbach, A. Nimberger, B. Markovskiy, E. Levi, E. Sominski and A. Gedanken, *Chem. Mater.* 14, 4155 (2002). <http://dx.doi.org/10.1021/cm021137m>
- [18] J. J. Ning, T. Jiang, K. K. Men, Q. Q. Dai, D. M. Li, Y. J. Wei, B. B. Liu, G. Chen, B. Zou and G. T. Zou, *J. Phys. Chem. C* 113, 14140 (2009). <http://dx.doi.org/10.1021/jp905668p>
- [19] Z. J. Wang, S. C. Qu, X. B. Zeng, J. P. Liu, F. R. Tan, Y. Bi and Z. G. Wang, *Acta Mater.* 58, 4950 (2010). <http://dx.doi.org/10.1016/j.actamat.2010.05.022>
- [20] B. Liu, J. H. Ma, H. Zhao, Y. Chen and H. Q. Yang, *Appl. Phys. A* 107, 437 (2012). <http://dx.doi.org/10.1007/s00339-012-6760-6>
- [21] J. Geurts, S. Rau, W. Richter and F. J. Schmitte, *Thin Solid Films* 121, 217 (1984). [http://dx.doi.org/10.1016/0040-6090\(84\)90303-1](http://dx.doi.org/10.1016/0040-6090(84)90303-1)
- [22] Y. Q. Guo, R. Q. Tan, X. Li, J. H. Zhao, Z. L. Luo, C. Gao and W. J. Song, *Cryst. Eng. Comm.* 13, 5677 (2011). <http://dx.doi.org/10.1039/c0ce00949k>
- [23] J. Q. Hu, X. L. Ma, N. G. Shang, Z. Y. Xie, N. B. Wong, C. S. Lee and S. T. Lee, *J. Phys. Chem. B* 106, 3823 (2002). <http://dx.doi.org/10.1021/jp0125552>
- [24] J. X. Wang, D. F. Liu, X. Q. Yan, H. J. Yuan, L. J. Ci, Z. P. Zhou, Y. Gao, L. Song, L. F. Liu, W. Y. Zhou, G. Wang and S. S. Xie, *Solid State Commun.* 130, 89 (2004). <http://dx.doi.org/10.1016/j.ssc.2004.01.003>
- [25] X. Wu, W. Cai and F. Y. Qu, *Chin. Phys. B* 18, 1669 (2009). <http://dx.doi.org/10.1088/1674-1056/18/4/065>
- [26] S. Y. Bae, J. Lee, H. Jung, J. Park and J. Ahn, *J. Am. Chem. Soc.* 127, 10802 (2005). <http://dx.doi.org/10.1021/ja0534102>
- [27] T. W. Kim, D. U. Lee and Y. S. Yoon, *J. Appl. Phys.* 88, 3759 (2000). <http://dx.doi.org/10.1063/1.1288021>